

Impact of Various Models on the Prediction of Spallation Residue Yields and Target Activation

L. DONADILLE*, A. BOUDARD, J.-C. DAVID, S. LERAY and C. VOLANT

DSM/DAPNIA/SPhN, C.E.A. Saclay, F-91191 Gif-sur-Yvette, France

Comparisons between the INCL4 cascade model, recently implemented in LAHET, and Bertini model are made in thin and thick lead targets. The impact of the cascade model used on the estimation of the target activity during its irradiation by a 1 GeV proton beam and its subsequent decay is discussed.

KEYWORDS: *cascade model; spallation residue; activity*

I. Introduction

The interest in spallation reactions has been renewed by the advent of the concept of accelerator-driven systems (see^{1,2}). Such devices couple an accelerator of particles with a thick target converter to create an intense neutron source, additionally surrounded by a subcritical assembly. The detailed design of these technological applications require powerful and reliable computational tools able to properly predict the production of particles and nuclides from the spallation target. For example, since most of the residual nuclides produced in the spallation target are radioactive, it is necessary to know their production rate in order to assess potential problems of activity or long-term radiotoxicity.

The spallation process is generally described by the coupling between an intra-nuclear cascade (INC), with an evaporation-fission model. The process ends up with the formation of a spallation residue in its ground state, or two fission products for heavy nuclei.

Recently, an improved version of the Liège intra-nuclear cascade (INCL4, see^{3,4}) has been developed. The new ingredients of this model are: (i) introduction of a smooth nuclear surface, (ii) a consistent dynamical Pauli blocking treatment, (iii) the division of the nucleons in participants and spectators, (iv) some improvements of the pion dynamics and (v) the extension to incident light clusters. The quality of the predictivity of the model, tested over a wide range of experimental data, has motivated its implementation in the LAHET Code System⁵. This offers the opportunity to perform consistent inter-comparisons of the Bertini⁶ and INCL4 cascade models using exactly the same evaporation code (here Dresner⁷), coupled with the Atchison fission model⁸) and particle transport conditions (simulated by LAHET). In all calculations presented hereafter, the Bertini cascade is coupled to the Multi-stage Preequilibrium Model (MPM, see⁹) as it gives more accurate results in this instance.

These comparisons, along with some confrontations to recent spallation residue experimental data corresponding to reactions in a thin ²⁰⁸Pb target, are made in Section I. In Section II the two cascades are compared for a thick ^{nat}Pb target. Section III is devoted to the estimation of the induced activity as given by both cascades and finally section IV contains our

conclusions and outlooks.

II. Residue production in thin target

The Bertini and INCL4 calculations for $p(1\text{ GeV}) + {}^{208}\text{Pb}$ are compared in **Fig. 1** with the experimental data of Refs.^{10,11}, measured in inverse kinematics.

As it has been already observed (see, e.g. Ref.¹⁰) the Bertini calculation overpredicts the yields of light spallation residues (around $A = 140$). This effect has been ascribed to a distribution of the excitation energy (E^*) too high at the end of the cascade, which results in evaporating more particles and finally producing lighter nuclides. As a consequence, this effect depletes the region of heavier residues around mass 190 which is underestimated. We see that INCL4 gives a much better reproduction of the spallation residue mass spectrum. However, part of the effects that we observe here may be due to the evaporation model, so conclusions regarding the cascade themselves must not be given too quickly since a different evaporation may lead to different results (see, e.g.^{4,10}). On the other hand, although fission is beyond the scope of this paper, we observe a large disagreement with both cascade models in this part of the spectrum. This is ascribed to the Dresner-Atchison model.

Regarding the isotopic distributions, shown here from lead down to terbium, two observations can be made: both cascades give very similar shapes, and the experimental data are poorly reproduced. The shape of the isotopic distributions is mostly driven by the neutron-proton competition in the evaporation stage of the reaction. This stage is treated by the same model (Dresner) for the two Bertini and INCL4 calculations, hence we have the same isotopic distribution shapes. Furthermore, the poor overall reproduction of the data is explained by a wrong description of the neutron-proton competition in Dresner.

III. Residue production in thick target

The results of calculations of residue production with a 1 GeV proton beam bombarding a thick cylindrical ^{nat}Pb target ($L = 100\text{ cm}$, $R = 10\text{ cm}$) are presented in **Fig. 2**. In this calculation the neutrons are transported with LAHET down to 20 MeV. On the mass distribution, it is clear that we observe much less different results for $A \geq 190$ between the two calculations than in **Fig. 1**. On the isotopic distributions,

* Corresponding author, Tel. (33-1) 69 08 72 77, Fax. (33-1) 69 08 75 84, E-mail: ldonadille@cea.fr

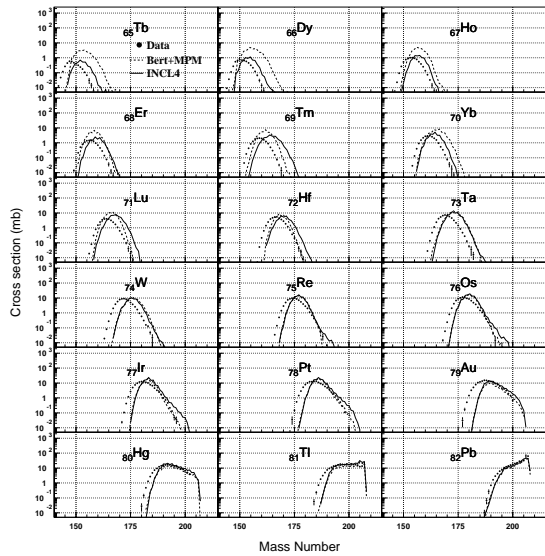
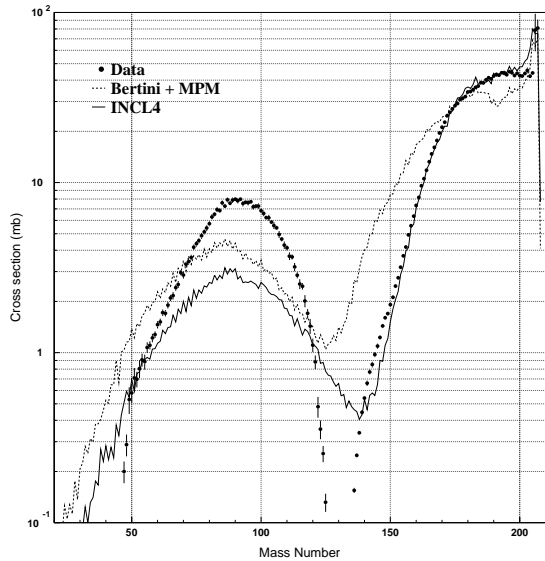


Fig. 1 Residue mass (top) and isotopic (bottom) production cross-sections for $p(1 \text{ GeV}) + {}^{208}\text{Pb}$ reactions. The predictions of the Bertini (+ MPM) and INCL4 cascades, coupled with the Dresner evaporation code are shown by the dashed and continuous lines, respectively. The data (dots), obtained in inverse kinematics, are from Refs.^{10,11}.

although the integrated production probability of a given element changes in correlation with the mass distribution, we see that the shapes are not influenced by the change of the target thickness. This is due to the fact that in a thick target many spallation reactions occur at lower energies than the initial beam energy. The **Fig. 3**, which shows the residue mass population for different energy bins of the particles inducing the reactions, illustrates this effect. We can observe that the majority of the residues in the region $A \geq 190$ are produced by reactions in between 20 and 300 MeV, which represent more than 60% of the total number of reactions, and it appears that the Bertini and INCL4 cascade models give similar results at low energy in this mass region. On the other hand, the nuclides

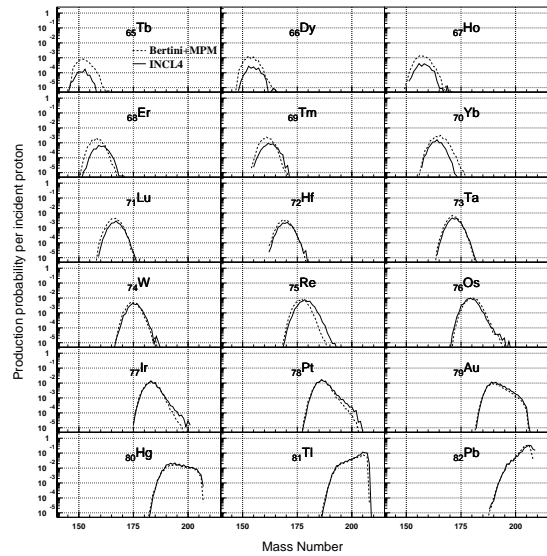
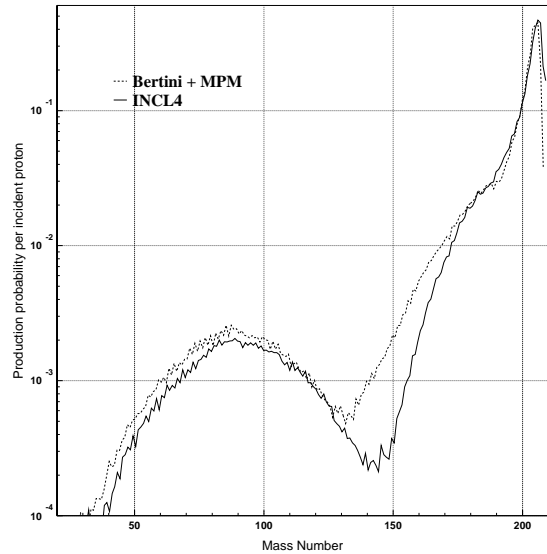


Fig. 2 Residue mass (top) and isotopic (bottom) production weights for p -induced reactions on a thick cylindrical ${}^{nat}\text{Pb}$ target ($L = 100 \text{ cm}$, $R = 10 \text{ cm}$) at 1 GeV incident energy. The weight is the formation probability per incident proton. The Bertini (+ MPM) and INCL4 calculations are shown by the dashed and continuous lines, respectively.

very far from the target ($A \simeq 150$), can only be produced from high energy interactions since high excitation energies are needed to have important mass loss by particle emission. The size of the target does not affect the isotopic distribution shapes because they are much more correlated to the evaporation model used than to the energy of the spallation reaction.

IV. Activation and decay estimations

We have estimated the activation due to the irradiation by the proton beam and the subsequent decay of the lead target. The ORIGEN2 code¹² has been used to calculate the evolution of the nuclides concentrations at a function of time. It uses

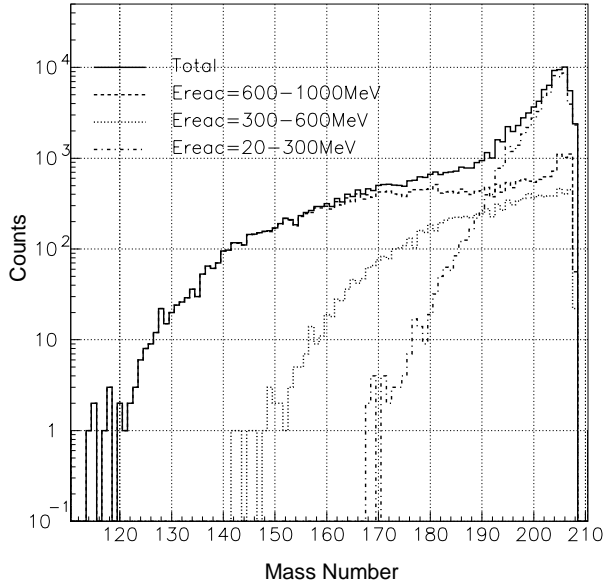


Fig. 3 Residue mass spectrum for p-induced reactions in a thick cylindrical ^{nat}Pb target ($L = 100$ cm, $R = 10$ cm) at 1 GeV incident energy. The calculation is performed with the Bertini code. Full line: total spectrum, dashed, dotted and dashed-dotted lines: reactions induced by particles of kinetic energy in the bin 600-1000 MeV, 300-600 MeV and 20-300 MeV, respectively.

the well known set of coupled differential equations depending on the individual decay constants, the neutron capture cross-sections, and the neutron flux.

A constant feeding rate F_i of a given isotope i can be introduced in the calculation. In our case, F_i (g/sec) = $C \times p_i \times I$ (mA), where C is a normalisation constant, p_i the production probability per incident proton of producing the i -th isotope, information taken from the result of the LAHET calculation, and I the intensity of the beam.

In this work, we did not take into account the neutron flux terms below 20 MeV, since only the neutrons beyond 20 MeV have been transported in LAHET, and the fission products have not been considered. Indeed, Shubin et al.¹³⁾ have estimated that the neutron flux below 20 MeV contributes to less than 10% to the total activity for decay times not larger than 10^8 days and that the fission products contribute to the order of 10-15%. Finally, we have limited the study to isotopes with production probability larger than 10^{-4} to keep the statistical uncertainty of the calculated results not larger than 14% relative. This means that we take into account about 300 nuclides with $A \geq 148$ and $Z \geq 64$

In **Figs. 4** and **5** are presented the activity estimations made from the Bertini and the INCL4 calculations, and **Table 1** gives the activity for some selected times. The primary proton beam has 1 GeV energy, 1 mA intensity and irradiates the cylindrical ($R = 10$ cm, $L = 1$ m) lead target. For both results and for a given time the main contributor to the total activity is plotted. During the irradiation phase one sees that the total activity

saturates at 5×10^5 Ci after about one month. This value is in good agreement with the Shubin et al. study¹³⁾. At this time the main contributors are ^{203}Pb and ^{206}Pb for the Bertini and INCL4 calculations, respectively. However, it can also be seen that these two nuclides contribute to less than an order of magnitude below the total activity. This means that in both cases a large number of different isotopes contribute almost equivalently to the total activity. A similar behavior is observed up to almost a month of decay, meaning that most of these nuclides have rather short periods ($T_{1/2} \leq 30$ d). For longer decay times the activity is due to only few long-lived nuclides. For example, after 10 years of decay the nuclide ^{204}Tl represents 60% of the activity, and after 10^4 years the dominant nuclide, representing 50% of the activity, is ^{202}Tl , populated by the β -decay of the long-lived ^{202}Pb . Finally one remarks that only the heaviest nuclides are the dominant ones.

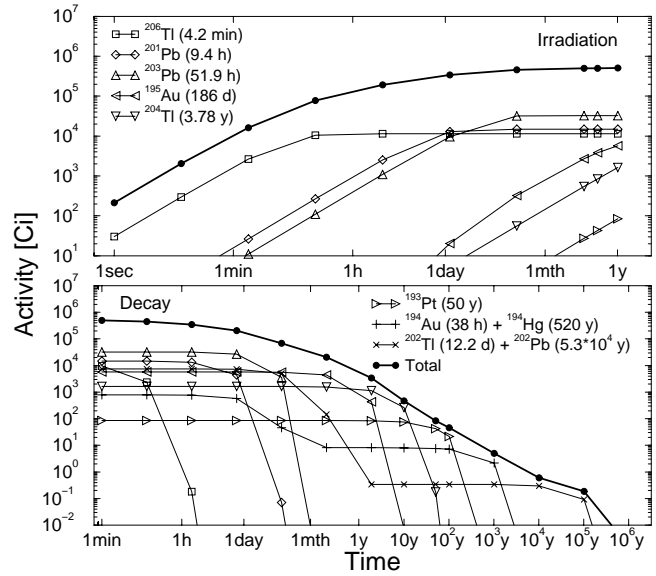


Fig. 4 Total and partial activities of a ^{nat}Pb target as a function of irradiation time (top) and cooling time (bottom) with the Bertini cascade model.

Table 1 Total activity (Ci) during the irradiation and decay phases given for some selected times.

	Irradiation time (sec)			
	10^3	10^5	10^7	3.2×10^7
Bertini	7.8×10^4	3.4×10^5	5.0×10^5	5.1×10^5
INCL4	7.5×10^4	3.4×10^5	4.8×10^5	4.9×10^5
	Decay time (sec)			
	6×10^4	6×10^7	3.2×10^8	3.2×10^{10}
Bertini	2.1×10^5	3.4×10^3	4.7×10^2	5.0
INCL4	1.9×10^5	3.5×10^3	5.6×10^2	5.4

On **Fig. 6** is shown the total activity ratio between the Bertini and INCL4 calculations. It can be observed that during the whole irradiation period and up to one year of decay the two models give activities consistent within 10%. It is in agreement with the previous observation of the fact that the

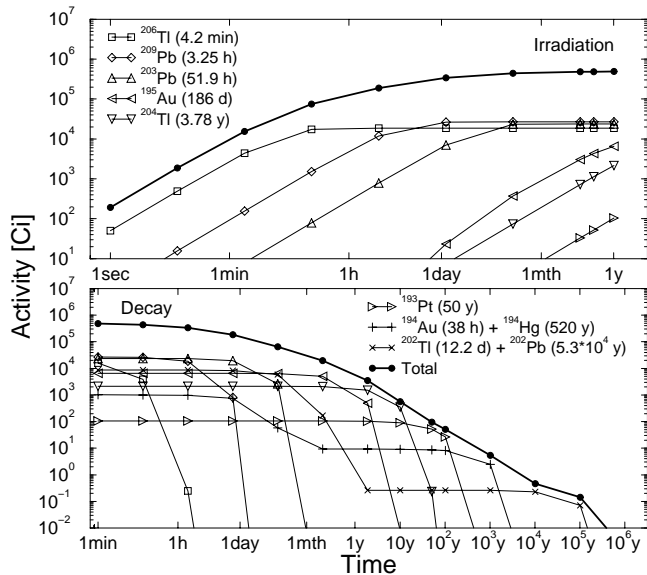


Fig. 5 Same as **Fig. 4** for a calculation with the INCL4 cascade model.

two cascade models give similar mass distributions in the case of such a thick target (see **Fig. 2**). However, some larger deviations can be seen between the two cascade models for longer decay times in **Fig. 6**. Since only few long-lived isotopes are left, the activity becomes very sensitive to the detailed of the isotopic distribution shapes and hence to the individual production probabilities. For example, the ratio of the production probabilities between the two cascade models is equal to 0.76 for ^{204}Tl and 1.32 for ^{202}Pb , very close to the corresponding ratio of activity after 10 and 10^4 years decay times at which this two nuclides are the dominant ones, respectively. The fact that no sensitivity is seen during the irradiation and for decay times smaller than one year is due to the coexistence of many short-lived nuclides which lead to compensation effects.

V. Conclusion and outlooks

Comparing results of with the Bertini (+ MPM) and INCL4 cascades, coupled to the Drener evaporation model in the LAHET code has shown that the activity in a thick lead target induced by a 1 GeV proton beam during the irradiation phase and up to 1 year of decay is insensitive (within 10%) to the cascade model. However, the sensitivity increases with decay time since the differences between the models become very close to the differences between the production probabilities of some specific long-lived isotopes (larger than 30% for ^{202}Pb).

This work is still in progress and we intend to investigate the impact of the evaporation model on the estimation of the activity. Indeed a different evaporation model will modify the shapes and mean values of the isotopic distributions. So it is expected to have a stronger impact than the one of the cascade model. In this aim the new KHS3v code¹⁴ is being implemented in LAHET. For these studies, the spallation residues together with the fission fragments will be taken into account, and since it has a non negligible effect for long decay times

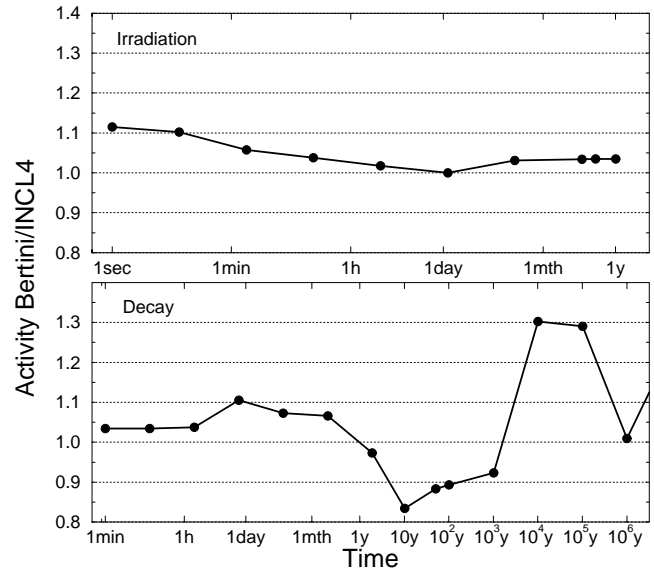


Fig. 6 Ratio of the activities given by the Bertini and INCL4 calculations, during the irradiation (top) and decay (bottom) phases.

($t \geq 10^5$ y, see¹³) the activation in the neutron flux with energy below 20 MeV will be considered as well.

Acknowledgment

We are grateful to R.E. Prael of the Los Alamos National Laboratory for providing us the LAHET3 source code and for his help. This work is supported by the HINDAS Collaboration, EU Contract N° FIKW-CT-2000-00031.

References

- 1) A.C. Bowman *et al.*, *Nucl. Instr. and Meth.*, **A 320**, 336 (1992).
- 2) C. Rubbia *et al.*, CERN/AT/95-44(ET) (1995).
- 3) J. Cugnon, C. Volant and S. Vuillet, *Nucl. Phys.*, **A 620**, 475 (1997).
- 4) A. Boudard, J. Cugnon, S. Leray and C. Volant, contribution to this conference and submitted to *Phys. Rev.*, **C**.
- 5) R.E. Prael and H. Lichtenstein, LANL Report LA-UR-89-3014 (1989), R.E. Prael, LANL Report LA-UR-01-1655 (2001), and private communication.
- 6) H.W. Bertini *et al.*, *Phys. Rev.*, **131**, 1801 (1963).
- 7) L. Dresner, ORNL Report ORNL-TM-196 (1962).
- 8) F. Atchison, in *Intermediate Energy Nuclear Data: Models and Codes, Proc. of a Specialists' Meeting*, OECD/NEA publications, Issy-les-Moulineaux, France, 199 (1994).
- 9) R.E. Prael and M. Bozoian, LANL Report LA-UR-88-3238 (1988).
- 10) W. Wlazlo *et al.*, *Phys. Rev. Lett.*, **84** (2000) 5736.
- 11) T. Enqvist *et al.*, contribution to this conference and *Nucl. Phys.*, **A 686**, 481 (2001).
- 12) A.G. Croff, *Nucl. Technology*, **62**, 335 (1983).
- 13) Yu.N. Shubin, A.V. Ignatyuk, A.Y. Konobeyev and V.P. Lunev, *Proc. Int. Conf. Evaluation of Emerging Nuclear Fuel Cycle System*, Global 1995, Sept. 11-14 (1995).
- 14) A.R. Junghans *et al.*, *Nucl. Phys.*, **A 629**, 635 (1998).